Anthropogenic aerosol depositions of nitrogen and phosphorus reduces the sensitivity of oceanic productivity to warming

Feng Zhou[1], Rong Wang[1,2], Yves Balkanski[2], Laurent Bopp[2], Philippe Ciais[2]

[1] Sino-France Institute of Earth Systems Science, Laboratory for Earth Surface Processes, College of Urban and Environmental Sciences, Peking University, Beijing, 100871, P.R. China, Email: zhouf@pku.edu.cn
[2] Laboratoire des Sciences du Climat et de l'Environnement, CEA CNRS UVSQ, 91191 Gif-sur-Yvette, France

Abstract
Satellite data reveal a strong link between contemporary oceanic productivity and climate. Models suggest oceanic productivity is reduced in response to enhanced water stratification induced by warming, but do not include the effect of increasing anthropogenic aerosol depositions of nitrogen and phosphorus (AAD). We model the response of oceanic productivity and chlorophyll to AAD, supported by *in situ* nutrient and chlorophyll measurements. As a result, AAD reduces the sensitivity of oceanic productivity to sea-surface temperature from -15.2±1.8 to -13.3±1.6 Pg C y^{-1}°C^{-1} in the stratified ocean during 1948-2007. The reduction over the North Atlantic, North Pacific and Indian oceans reaches 40, 24 and 25%, respectively. We hypothesize that future reduction of aerosol emissions in response to higher air-quality standards will accelerate the decline of oceanic productivity per unit warming.

Key Words
Climate warming, modelling, nitrogen deposition, phosphorus deposition

Introduction
Marine net primary production (NPP) is a critical component of the Earth's carbon cycle, transferring some 50 Pg of carbon from the atmosphere to the ocean each year (Li et al., 2016). Yet, field studies and model simulations indicate a decline in oceanic NPP during 1998-2010 and likely throughout the 20th century too. The decline is attributed mainly to the increasing thermal stratification of the water column, caused by rising sea-surface temperature. This increase in stability reduces the supply of nutrients from subsurface waters, thereby inhibiting the growth of phytoplankton. The process is simulated by ocean biogeochemical models, and is expected to continue further, reducing marine NPP. In contrast, anthropogenic aerosol deposition (AAD) adds nutrients to the oceanic surface water, which should promote NPP. Previous studies suggest that anthropogenic nitrogen (N) deposition alone enhances the global oceanic NPP by 0.3 Pg C y^{-1}. Here, we estimate the effect of AAD, including N, iron (Fe) and phosphorus (P) on the evolution of oceanic NPP for the varying climate of the past 60 years.

Methods
Atmospheric depositions of nutrients
Emissions of N_r include nitrogen oxides and ammonia from combustion, and agriculture and natural soil and oceanic sources (Zhou et al., 2015; 2016). Emissions of P and Fe from combustion estimated for 1960-2007 were extended to 1850-2010 based on sulfer emissions in ACCMIP. Other natural sources, including dust, biogenic particles, volcanoes and sea-salt were assumed to be constant – isolating the direct anthropogenic component. Emissions of P and Fe were converted to PO_4 and soluble Fe (sFe), which are bio-available, using prescribed ratios. Emissions of N_r, PO_4 and sFe were prescribed in the LMDZ-OR-INCA atmospheric transport chemistry model to obtain the oceanic deposition of dissolved inorganic N (DIN, including nitrate and ammonium), PO_4 and sFe in 1850 and for annual snapshots every 10 years from 1960 to 2010.

Modeling systems
Monthly fields of DIN, PO_4 and sFe deposition were applied to the oceanic biogeochemical model NEMO-PISCES (version 2). NEMO-PISCES captures the observed response of oceanic NPP to both dust (*19*) and climatic variability. We ran the model over the period 1768-2007 using the first 180 years as a spin-up. We ran two simulations to study the impact of AAD: a control simulation (CTL) with DIN, PO_4 and sFe deposition fixed at the 1850 levels, and an experimental simulation (DEP) with deposition varying from 1850 to 2007, interpolated from the snapshot simulations (*13*). The difference between the DEP and CTL outputs was considered as the response to AAD.

Results

Model performance. The spatial pattern of modeled NPP is comparable to satellite-based estimates for 1997-2007. The period covered by satellite observations is relatively short and corresponds to an era of intense anthropogenic aerosol emissions, making it difficult to detect the effect of AAD on marine NPP from space. We instead evaluated our model using *in situ* Chl measurements from 1948 to 2007. The oceanic level of Chl does not have a simple relationship with NPP, but Chl levels and the rate of carbon fixation by phytoplankton both co-vary in response to environmental drivers. Chl concentration is thus a valid indicator of oceanic NPP. We assembled a total of 182 552 measurements of Chl concentrations over the global oceans. Modeled Chl concentrations match the majority of observations around the 1:1 line. We identified the sites affected by AAD by comparing the modeled and observed Chl data for the sites (n = 19 011) where the relative difference between DEP and CTL is >10% (**Figs. 1A-B**). Including AAD decreases the normalized mean bias (NMB) and root mean square deviation (RMSD) from -42% and 0.24 to -32% and 0.17, respectively. Nutrients and Chl in the oceans are evidently influenced by factors other than AAD, including ocean physics and other external factors such as interaction with sediments, river inputs, hydrothermalism and deposition of natural dust. The spatio-temporal distribution of Chl responds to changes in all these factors.

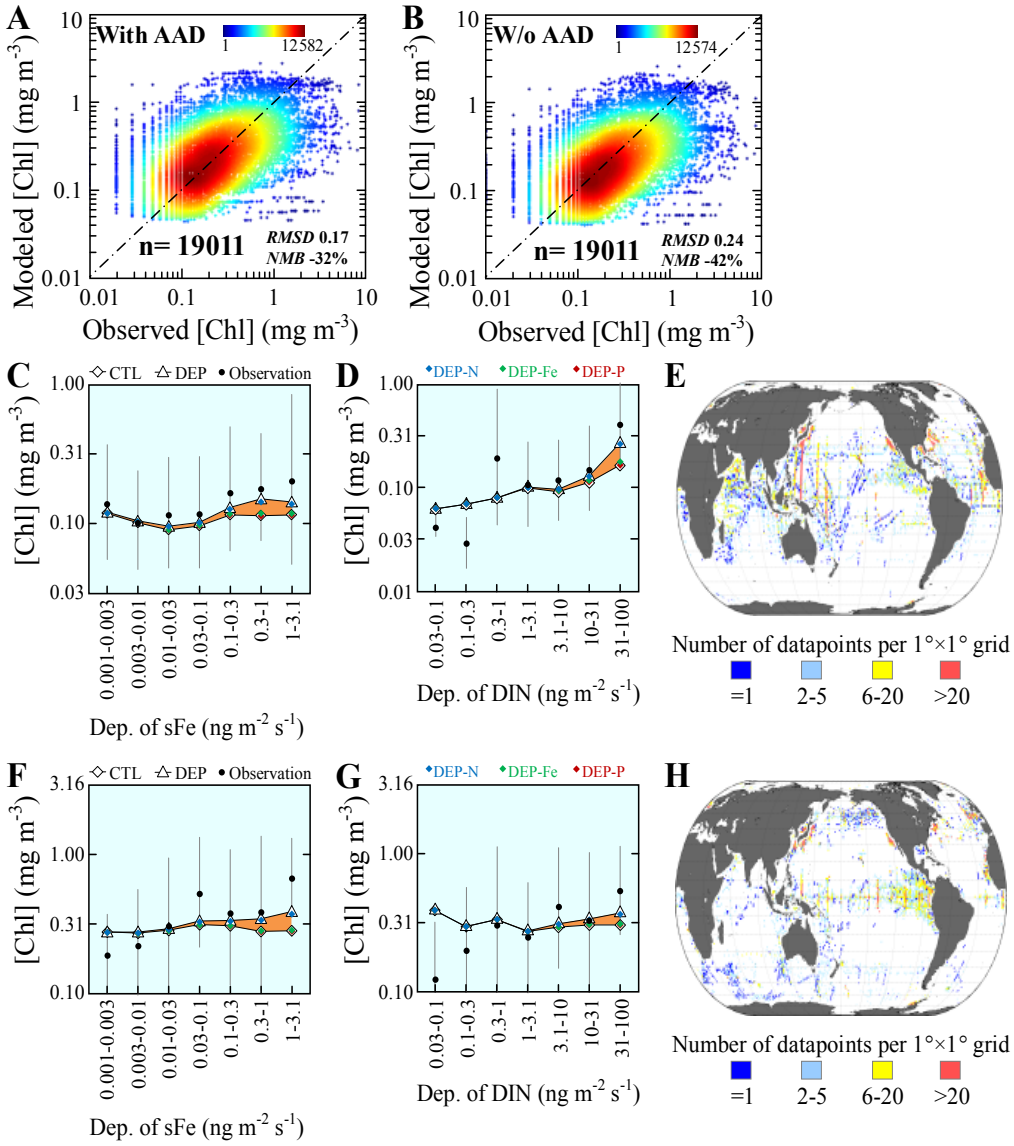

Figure 1. Impact of AAD on Chl concentrations. (A-B) Comparison of modeled and observed Chl concentrations with or without (w/o) AAD, at sites where the impact of AAD on modeled Chl is >10%. Plots are made using a log scale, with colors indicating the density of data points in the panel. Number of sites (n), normalized mean bias (NMB) and root mean square deviation ($RMSD$) are shown. (C-H) All Chl sites (n = 182 552) are divided into four quartiles of Chl modeled without AAD. The modeled Chl in the first (C, D) and second (F, G) quartiles are plotted against anthropogenic deposition (Dep.) of sFe (C, F) and DIN (D, E) and compared with the observations (solid circles). Chl concentrations are averaged at an interval of 0.5 of ($\log_{10}$) deposition. The grey-shaded areas show the difference of Chl concentrations modeled with (open triangles, DEP) or without (open diamonds, CTL) AAD. The modeled Chl with anthropogenic deposition of N only (DEP-N), Fe only (DEP-Fe) or P only (DEP-P) are shown as

blue, green and red diamonds, respectively. Error bars show standard deviations of observed Chl. (E) Distribution of sites in (C-D). (H) Distribution of sites in (F-G).

To isolate the response of Chl to AAD, we regrouped all Chl measurements at open-ocean sites into four quartiles of Chl modeled without AAD. In the first and second quartiles, the sites are more oligotrophic and sensitive to nutrient addition by AAD than those in the third and fourth quartiles. We plotted the Chl concentrations in the first and second quartiles against anthropogenic deposition of DIN or sFe (**Figs. C-H**). The impact of AAD on Chl is shown as a shaded area. The modeled Chl concentrations at high deposition sites agree better with the observations, consistent with an effect of AAD on Chl levels. Furthermore, sensitivity simulations with anthropogenic deposition of only N or P or Fe (diamonds in **Figs. C-H**) show that the effect of N is dominant, followed by Fe, and very weak for P. The impact of AAD is small, suggesting that factors other than AAD dominate the variability of Chl.

Modeled PO_4, DIN (only nitrate) and sFe concentrations with or without AAD were also compared against *in situ* measurements, including 170 588 observations of nitrate, 438 240 of PO_4 and 214 of sFe. Measurements of nitrate and PO_4 concentrations below the detection limits of 0.1 mmol m^{-3} for nitrate and 0.03 mmol m^{-3} for PO_4 were not kept, and we thus compared the modeled and observed nitrate and PO_4 above a threshold. The RMSD and NMB for (log_{10}) nitrate decreased from 0.61 and -56% without AAD to 0.56 and -46% with AAD, respectively. The RMSD for (log_{10}) PO_4 increased slightly from 0.45 to 0.46 with AAD. Detecting the impact of AAD on PO_4 requires further discrimination of reactive and non-reactive P in the model and data. The RMSD and NMB for (log_{10}) sFe decreased from 0.63 and -68% to 0.57 and -63%, respectively.

Behrenfeld et al. (2006) found an inverse relationship of increasing sea-surface temperature (SST) with decreasing NPP in the permanently stratified oceans from 1999 to 2004. We observed a similar relationship in our simulations when comparing the period from 1948-1977 to 1978-2007. Furthermore, the correlations are equally as high with or without AAD (**Fig. 2**), but including AAD decreases the sensitivity of NPP changes to SST changes. The sensitivity of modeled NPP to SST decreased from -15.2±1.8 to -13.3±1.6 Pg C y^{-1} $°C^{-1}$ with AAD, a reduction by +1.9 Pg C y^{-1} $°C^{-1}$ or 12.5% relative to that without AAD. The North Pacific has the largest change of the slope from -2.56±0.46 to -1.96±0.40 Pg C y^{-1} $°C^{-1}$. Sensitivity in the North Atlantic decreases by 40% (-0.35±0.10 to -0.21±0.10 Pg C y^{-1} $°C^{-1}$), the largest percentage change. Our finding has two implications. First, any observation-based techniques to detect the influence of global warming on oceanic NPP have to take into account the role of AAD, as human-emitted aerosols can partly offset the effect of anthropogenic warming. Second, the evolution of AAD has to be considered when using the model to predict future oceanic NPP.

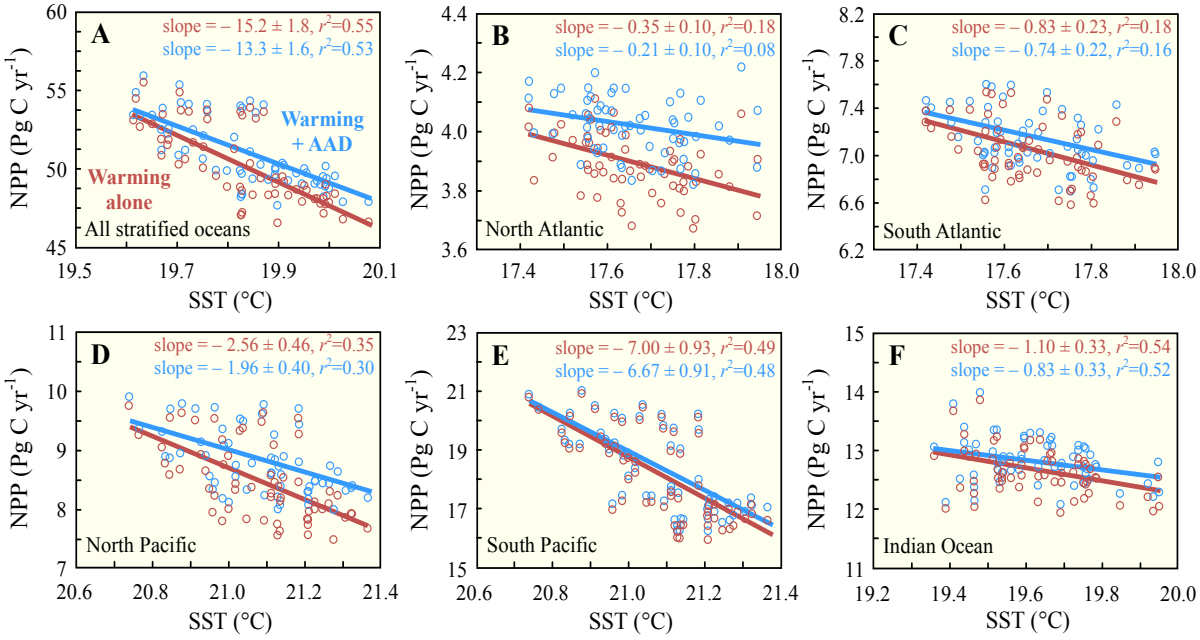

Figure 2. Relationship between net primary production (NPP) and annual mean sea-surface temperature (SST) for 1948-2007. The NPP is computed from the ocean model and SST is from the observations (*13*). The permanently stratified oceans (A) as defined by Behrenfeld et al. (2006) are divided into (B) North Atlantic, (C) South Atlantic, (D) North Pacific, (E) South Pacific and (F) Indian Oceans. The circles show the

relationship between NPP and SST under warming alone (red) or warming and AAD together (blue). The sensitivity of NPP to SST (Pg C y^{-1} °C^{-1}) and coefficient of determination (r^2) are estimated from least-squares regression analysis.

Limitations. Our estimate is subject to several sources of uncertainty. First, we accounted for direct emissions of sFe but not for indirect conversion of insoluble Fe to sFe in dust and combustion particles by anthropogenic acids. Second, we did not account for the emission of dust from land cover change. Third, the monthly resolution of AAD did not capture episodic transport, so our model cannot predict algal blooms. Fourth, we did not include the toxic effect of heavy metals contained in large particles, although their impact is limited to coastal areas due to the short atmospheric residence time of large particles.

Conclusion and remarks

Ocean ecosystems are sensitive to environmental changes. Global warming induced by emissions of anthropogenic greenhouse gases has increased ocean stratification and reduced the nutrient supply for phytoplankton from oceanic circulation. Our study identifies deposition of anthropogenic aerosols as an overlooked factor that can partly offset the decline of nutrients. However, ambient aerosol pollution led to ~3 million human premature deaths in 2010, so these emissions will inevitably be controlled, likely before 2030 in the major emitting countries. According to the Representative Concentration Pathways scenarios, the emissions of nitrogen oxides and sulfur (sharing similar sources as P and Fe) will decrease by 34-59% and 75-88% from 2010 to 2100, although ammonia emissions will increase by 3-55%. If our analysis proves robust, higher air-quality standards, while improving air quality, will reduce AAD and accelerate decline in marine NPP due to ocean warming. Such changes will have impacts on marine food webs, and the global carbon and nitrogen cycles and climate.

References

Li B, Gasser T, Ciais P, Piao S, Tao S, Balkanski Y, Hauglustaine D, Boisier JP, Chen Z, Huang M, Li LZ, Li Y, Liu HY, Liu JF, Peng SS, Shen ZH, Sun ZZ, Wang R, Wang T, Yin GD, Yin Yi, Zeng H, Zeng ZZ, Zhou F (2016). The contribution of China's emissions to global climate forcing. Nature 531(7594), 357-361.

Zhou, F; Ciais, P; Hayashi, K; Galloway, J; Kim, D-G; Yang, C; Li, S; Liu, B; Shang, Z; Gao, S (2016). Re-estimating NH_3 emissions from Chinese cropland by a new nonlinear model, Environmental Science & Technology 50, 564-572.

Zhou F, Shang Z, Zeng Z, Piao S, Ciais P, Raymond PA, Wang X, Wang R, Chen M, Yang C, Tao S (2015). New model for capturing the variations of fertilizer‐induced emission factors of N_2O. Global Biogeochemical Cycles 29(6), 885-897.

Behrenfeld, M. J.; O'Malley, R. T.; Siegel, D. A.; McClain, C. R.; Sarmiento, J. L.; Feldman, G. C.; Milligan, A. J.; Falkowski, P. G.; Letelier, R. M.; Boss, E. S. (2006), Climate-driven trends in contemporary ocean productivity, Nature, 444, 752–755